LASER ULTRASONIC MODELLING FOR NDT APPLICATIONS

Damien SÉGUR [1]
[1] CEA-LIST, Toulouse, France
damien.segur@cea.fr

Abstract. The Laser ultrasonic technique (LUT) is an interesting method to perform inspection of large aeronautical panels of complex shapes. Its non-contact feature avoids coupling problems and could improve the efficiency of the NDT inspection in the composite manufacturing industry. If the ultrasound generation process is well understood in metallic samples, the application of the technique in composite parts is more complex. Semi-analytical and numerical models are implemented to describe the ultrasonic generation in metallic and composites materials. A detailed description of the ultrasonic source due to the laser radiation absorption in the material is provided according to suitable parameters.

Introduction

Laser ultrasonics deals with the generation and detection of ultrasound in a solid medium using laser beam. Typically, the technique uses laser irradiation to induce ultrasound by either ablating the medium or using rapid thermal expansion. The resulting ultrasonic wave packets are also typically measured using optical probes. Laser ultrasonics therefore provides a noncontact way of carrying out ultrasonic interrogation of a medium to provide information about is properties. Laser ultrasonic measurement systems are particularly attractive to nondestructive structural and materials characterization of solids because they are noncontact leading to increased speed of inspection, have a very small footprint and can be operated on curved surface and are broadband systems providing information from the kHz to the GHz range. In this article, the basis of the laser ultrasonic technique as related to nondestructive characterization of solid materials is discussed. The basic process of laser generation of ultrasound is described and a promising modelling approach has been investigated. It consists in a fully numerical approach of the thermoelastic problem that allows simulating the multi-stacking structure of composite parts with complex shape.

1 Laser Ultrasonic Testing

Recently laser-generated ultrasound has been extensively exploited for characterizing materials. The application of laser ultrasonic has received considerable attention in a wide range of non-destructive evaluation (NDE) of structures [1] such as cracks detection, measuring bulk material properties and detecting disbands in laminated materials, coated materials or in adhesively bonded assemblies.

1.1 Principle of the technique

A pulsed laser beam impinges on a material and is partially absorbed by it. The electromagnetic power that is absorbed by the material is converted to heat, leading to rapid localized temperature increase. Ultrasonic waves can be generated by two mechanisms depending upon the power density of the laser incident beam. At high energy density, a thin surface layer of the solid material melts, followed by an ablation process whereby particles fly off the surface, thus giving rise to forces which generate the ultrasonic waves. At low energy density, the surface material does not melt, but it expands at a high rate and wave motion is generated due to thermoelastic processes. For applications in non-destructive testing (NDT), ultrasound generated by laser irradiation in the thermoelastic regime is of interest.

It is important to characterize the ultrasound generated by laser heating of a material in order to determine the amplitude, frequency content, and directivity of the generated ultrasonic beam. If the material ablates, the ultrasound that results from momentum transfer can be modelled as arising from a normal impulsive force applied to the surface. Analytical solutions to this problem can be obtained by appropriate temporal and spatial convolution of the elastodynamic Green function (solution for an impulsive point force on a half-space) [2]. For thermoelastic generation on materials such as metals where the light energy is absorbed in a very thin layer on the surface, Scruby [3] argued that the relevant elastodynamic problem is that of shear dipoles acting on the surface of the sample. His argument was based on the consideration that a point expansion source in the interior of a solid can be modelled as three mutually orthogonal dipoles and this degenerates into a pair of orthogonal dipoles as the expansion source moves to a free surface. This approach was given a rigorous basis in the form of a surface centre of expansion model proposed by Rose [4] and further developed by Spicer [5]. McDonald [6] and Sanderson [7] improved this model, taking into account both thermal diffusion and the finite spatial and temporal shape of the laser pulse on metals. Usually, optical detection system measures the normal displacement at the surface of the sample. It corresponds to the most common laser interferometric detection [8].

1.3 Governing equations

The governing equations of the generalized thermoelasticity in the linear elastic case are given by the coupled heat conduction and wave equations describing the coupling of displacement and temperature fields. In the present work a 2D case with plane-strain boundary conditions is investigated, which is a good approximation of a line-focused laser source. The hyperbolic heat equation is given as:

$$\rho c_v\,(T)(\,\dot{T} + \tau\ddot{T}) = \boldsymbol{\nabla}^2(\kappa(T).T) + q + \tau\dot{q} - T_0\,\boldsymbol{\beta}\,\boldsymbol{\nabla}\dot{\boldsymbol{u}} \qquad (1)$$

Where $T = T(\boldsymbol{r}, t)$ denotes the temperature, κ the thermal conductivity, c_v the specific heat of the material at constant deformation, T_0 the ambient temperature, $q = q(\boldsymbol{r}, t)$ the external heat flux, ρ the density, $\boldsymbol{\beta}$ the thermal moduli, $\boldsymbol{u}$ the displacement, τ the thermal relaxation time and the dot symbol corresponds to the time derivative.

Substituting the constitutive law $\boldsymbol{\sigma} = [\boldsymbol{C}]\!:\boldsymbol{\nabla u}$ and the thermal stresses $\boldsymbol{\sigma_T} = [\boldsymbol{C}]\!:[\alpha]\boldsymbol{\nabla T}$ in the equilibrium law $\boldsymbol{\nabla}\cdot\boldsymbol{\sigma} = \rho\ddot{\boldsymbol{u}}$ gives the wave equation with a term source in the right hand side:

$$\boldsymbol{\nabla}\cdot([\boldsymbol{C}]\!:\boldsymbol{\nabla u}) - \rho\ddot{\boldsymbol{u}} = [\boldsymbol{C}]\!:[\boldsymbol{\alpha}]\,\boldsymbol{\nabla T} \qquad (2)$$

where $[\boldsymbol{C}]$ and $[\boldsymbol{\alpha}]$ stand for the stiffness tensor and the thermal dilatation tensor respectively. For simplicity a fully decoupled linear analysis for homogeneous, isotropic materials is considered. The basic problem of thermoelastic generation of ultrasound can be decomposed into three sub problems: (1) electromagnetic energy absorption by the medium, (2) the consequent thermal diffusion problem with heat sources due to the electromagnetic energy absorbed, (3) and the resulting elastodynamic problem with volumetric sources due to thermal expansion. The temperature increase is assumed not to change the elastic, electromagnetic, or thermal properties. And the mechanical displacement is assumed not to alter the thermal profile of the material.

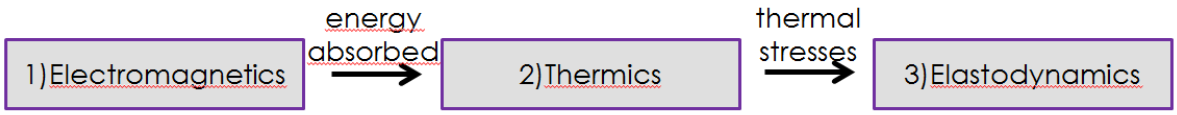

For given boundary conditions, the solution of the wave equation can be calculated analytically [10] or by numerical methods as described in this article. Since the temperature field induces the stress and displacement fields and the effect of the displacement fields on the temperature field is assumed negligibly small, the sequential field coupling is used. First, the Finite integration technique is used to simulate the temperature field. Then, the displacement fields are simulated using a finite difference time-domain solver.

3. Numerical scheme for solving the thermoelastic equations in laser ultrasonics

3.1 Finite Integration Technique (FIT) for solving the heat equation

Hereafter, we propose a discrete formulation for the heat equation. The starting point for the discrete formulation is the energy conservation equation in a finite volume V

$$\int_V \rho c_P \frac{\partial T}{\partial t} dV = \int_V \frac{\partial Q_s}{\partial t} dV - \oint_{\partial V} \mathbf{J} \cdot d\mathbf{s} \qquad (3)$$

Where ρ is the density of the material (in kg m^{-3}), c_p the mass heat capacity (in J kg^{-1} K^{-1}), T the absolute temperature (in K), Q_s the heat source (in J kg^{-1}) and $\mathbf{J}$ the flux thermal density. This latter is related to the thermal field by the Fourier's law:

$$\mathbf{J} = -\kappa \nabla T, \qquad (4)$$

with κ the thermal conductivity of the material (in W m^{-1} K^{-1}).

To discretize the equations (3) and (4), we define in the domain problem a system of grids of the Yee type that are orthogonal and shifted as be shown in **Pic. 1**. By convention, the two grids are called the primary grid (solid black lines **Pic. 1**) and the secondary grid (dashed red lines in **Pic. 1**) respectively.
In the FIT numerical scheme, all the scalar variables will be associated to the nodes of the primary grid whereas the secondary variables will be associated to the primary grid edges and to the facets of the secondary grid. The exact definition of the state variables will be given later.

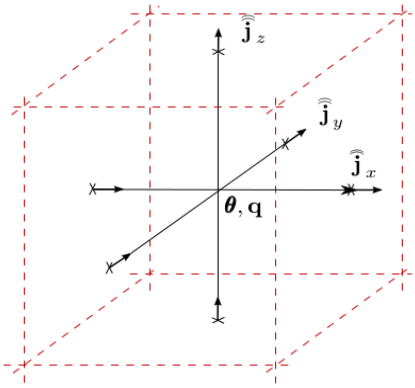

Pic. 1. *System of the grids used in discretizing the conservation and the Fourier's laws. The solid black lines show the edges of the primary grid and the dashed red lines show the edges of the secondary one.*

Expressing the equation (3) in a cell of the secondary grid give us

$$\frac{\partial}{\partial t}\int_{\tilde{V}_i} \rho c_P T dV = \int_{\tilde{V}_i} \dot{Q}_s dV \qquad \oint_{\partial \tilde{V}_i} \mathbf{J}\cdot d\mathbf{s}. \tag{5}$$

Integrating the equation (4) in a flux tube from the nodes *i* et *j* give us

$$\int_{L_{ij}} \kappa^{-1} dl \int_{A(l)} \mathbf{J}\cdot d\mathbf{s} = \int_{A_i} T ds - \int_{A_j} T ds. \tag{6}$$

Then we expand T and $\mathbf{J}$ in Taylor series around the centre of cell of the primary grid $\mathbf{r_i}$ and the centre of the edge l_i respectively

$$T(\mathbf{r}) = T(\mathbf{r}_i) + \nabla T_{\mathbf{r}_i}\cdot \Delta\mathbf{r} + \mathcal{O}\left(\Delta\mathbf{r}^2\right), \tag{7}$$

$$\mathbf{J}(l) = \mathbf{J}(l_{i'}) + \partial_l \mathbf{J}|_{l_{i'}}\cdot \Delta l + \mathcal{O}\left(\Delta l^2\right), \tag{8}$$

Applying (7) and (8) in (5) and (6) keeping only the first order terms give us

$$\frac{\partial T_i}{\partial t}\int_{\tilde{V}_i} \rho c_P dV \approx \int_{\tilde{V}_i} \dot{Q}_s dV - \oint_{\partial \tilde{V}_i} \mathbf{J}\cdot d\mathbf{s}. \tag{9}$$

$$\int_{A_{i'}} \mathbf{J}_{i'}\cdot d\mathbf{s} \int_{L_{ij}} \kappa^{-1} dl \approx T_i \Delta A_i - T_j \Delta A_j, \tag{10}$$

with $\mathbf{J_{i'}}=\mathbf{J}(\mathbf{r_i})$ et $T_i=T(\mathbf{r_i})$ where $\Delta A_{i'}$ is the oriented surface element. One can note that in the case of the material is homogeneous in the secondary cell and along the corresponding edges, the second order approximation is implemented to prevent the cancelation of the first order after the integration.

We define the state variable as following

$$\theta_i := T_i \tag{11}$$

$$\hat{\mathbf{j}} := \int_{A_{i'}} \mathbf{J}_{i'}\cdot d\mathbf{s}, \tag{12}$$

The temperature of the primary cell nodes and the thermal flux through the facets of the

secondary grid. We define also the material matrices as

$$\mathbf{M}_c := \int_{\tilde{V}_i} \rho c_P dV \qquad (13)$$

$$\mathbf{M}_\kappa^{-1} := \int_{L_{ij}} \kappa^{-1} dl \qquad (14)$$

Applying (9) and (10) in all the secondary cells and using the topological operators of the FIT method [9, 10], we obtain the following system of equations

$$\mathbf{M}_c \dot{\boldsymbol{\theta}} = \dot{\mathbf{q}} - \widetilde{\mathbf{S}}\widehat{\mathbf{j}} \qquad (15)$$

$$\mathbf{M}_\kappa^{-1}\widehat{\mathbf{j}} = -\mathbf{G}\boldsymbol{\theta}, \qquad (16)$$

which after eliminating the thermal flux term give us the following equation

$$\widetilde{\mathbf{S}}\mathbf{M}_\kappa\mathbf{G}\boldsymbol{\theta} - \mathbf{M}_c\dot{\boldsymbol{\theta}} = -\dot{\mathbf{q}} \qquad (17)$$

That is the discrete formulation of the heat equation.

The formulation (17) is an initial values problem. To resolve it, we discretize the thermal derivative with a finite difference scheme.

$$\frac{df(t)}{dt} \approx \frac{f(t+\Delta t) - f(t)}{\Delta t} \qquad (18)$$

The time axis t is discretized with a homogeneous grid $t_n = n\Delta t$, $n = 0, 1, \ldots, N_t$ and we apply (18) in (17). The latter becomes

$$\left(\widetilde{\mathbf{S}}\mathbf{M}_\kappa\mathbf{G} - \frac{\mathbf{M}_c}{\Delta t}\right)\boldsymbol{\theta}_{n+1} = \frac{\mathbf{M}_c}{\Delta t}\boldsymbol{\theta}_n - \dot{\mathbf{q}}_n \qquad (19)$$

Starting from the initial value of the thermal field $\boldsymbol{\theta_0}$ we iterate in the time and at each $n+1$ time step, we evaluate the temperature $\boldsymbol{\theta_{n+1}}$ from the value at the previous time step $\boldsymbol{\theta_n}$. One can remark that (19) is an implicit scheme, i.e. the following value $\boldsymbol{\theta_{n+1}}$ is obtained resolving a system of linear equations.

3.2. Numerical example and validation

The FIT formulation defined above is applied to the resolution of a 1D problem for validation purpose. Let us consider an aluminum plate located in two temperature fields of constant temperature equal to 50°C and 100°C respectively. The physical parameters of the aluminum plate are $\rho = 2707$ kg m^{-3} for the density, $c_p = 0.897$ J kg^{-1} K^{-1} for the heat capacity and $\kappa = 237$ W m^{-1} K^{-1} for the thermal conductivity. We consider that the initial temperature of the plate is 0°C.

Pic. 2 (left) shows the evolution of the thermal equilibrium at the center of the plate. The FIT solution (in green) is compared to the analytical solution (in blue). Excellent agreement is obtained between these two models. **Pic. 2** (right) represents the temperature profile inside the plate after the plate was located in the two thermal fields. Excellent agreement is also obtained justifying that the solution of the heat equation by the FIT model is valid.

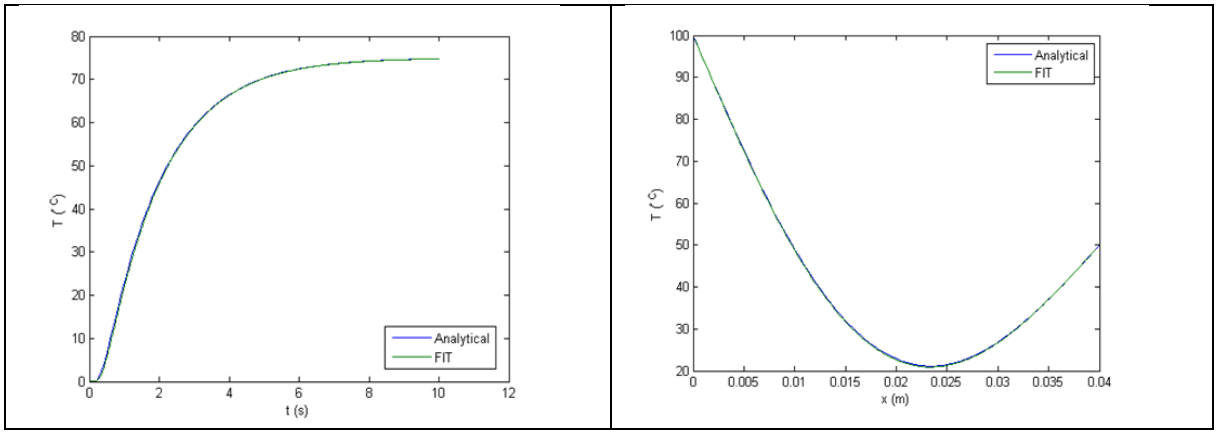

Pic. 2. *Comparison between the analytical solution (in blue) and the FIT solution (in green) for (a) the evolution of the temperature at the centre of the plate and (b) the thermal profile within the plate after 1s.*

As a second validation example, let us consider the same plate that is located in the air. Physical parameters of the air are $\rho = 1.1843$ kg m^{-3}, c_p=1.005 J kg^{-1} K^{-1} and $\kappa = 0.02454$ W m^{-1} K^{-1}. Boundary conditions are a Dirichlet conditions (constant temperature at one boundary of the plate). We locally excite the plate with a heat pulse of 500ms at the surface of the plate. **Pic. 3** reports the temperature distribution in the plate and in the air at several times: 1, 1.2, 2 and 5s.

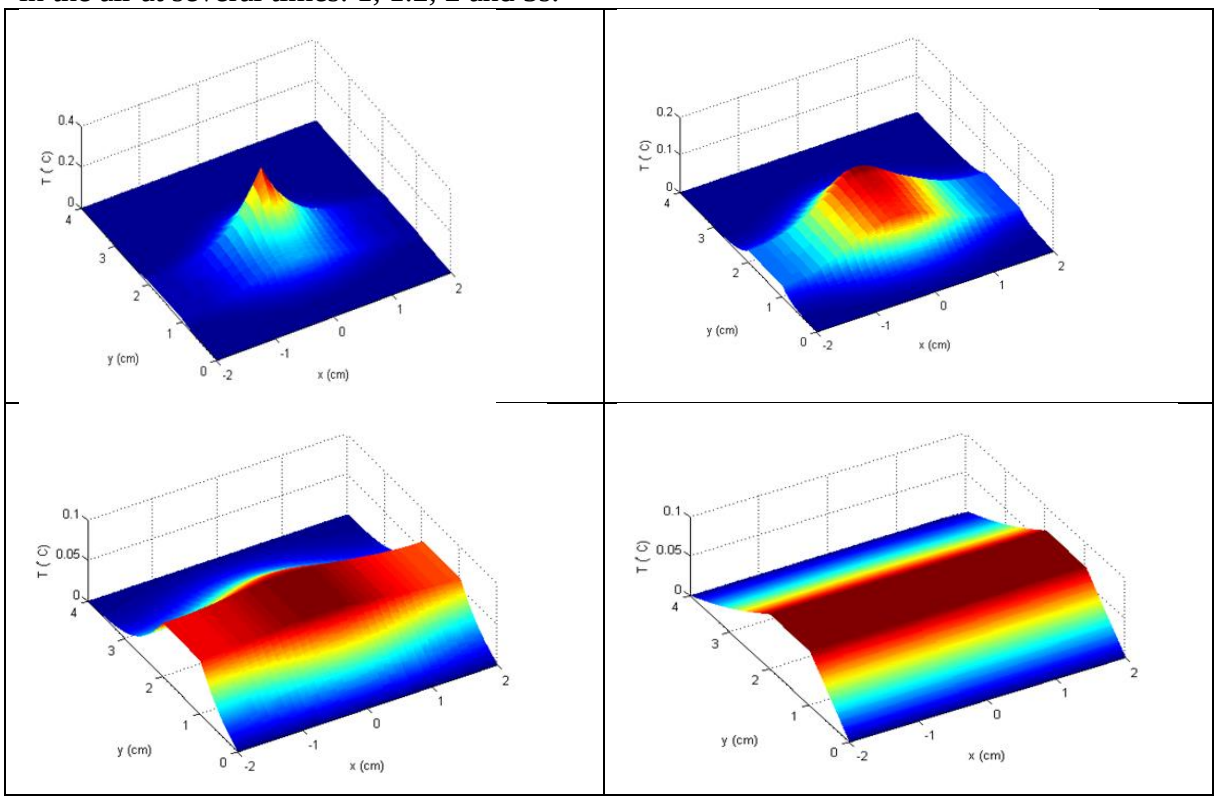

Pic. 3. *Evolution of the thermal field inside the plate at different times: 1, 1.2, 2 et 5 s (from left to right and top to bottom).*

3.3 Finite Difference Time Domain scheme for solving the wave equation

A numerical code has been developed by Airbus, in order to simulate ultrasonic propagation within flat or curved composites. This code aims at simulating inspection of complex (geometry and inner structures) composite parts such as anisotropic parts with account of the rotation of the crystallographic orientation within curved composites (for instance stiffeners). To deal with these complex and mixed phenomena Airbus Group Innovations has developed numerical codes with a Finite Difference in Time Domain (FDTD) scheme on staggered grids in space and leap-frog in time. The implemented model is a stress-velocity scheme proposed by Virieux, which is depicted below in **Pic. 4**:

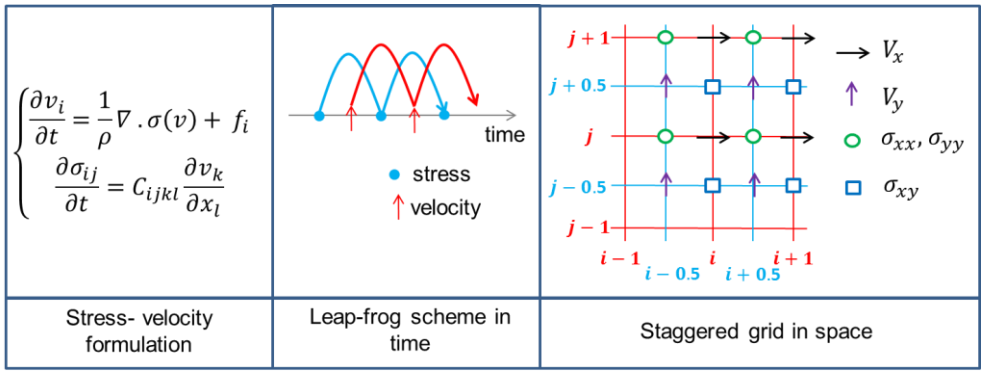

Pic. 4. *FDTD numerical scheme.*

This model considers a propagation medium in which the local material properties are associated to the corresponding cells of the mesh. This allows description of strongly heterogeneous and anisotropic materials such as curved composites with waviness. A Perfectly Matched Layers (PML) model is implemented for the boundary conditions to simulate non-reflective boundaries. **Pic. 5** below illustrates the CIVA/FDTD hybrid code for composites which has been developed through the project; this picture shows the curved composite (multi-layered composite parts) and also includes two different flaws: ply waviness, as well as a planar flaw, which are representative of main composite damages.

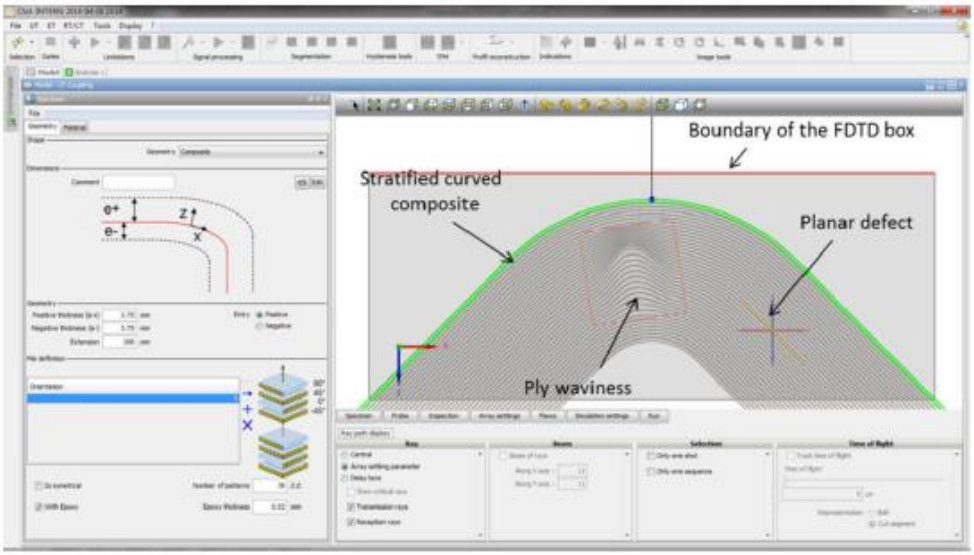

Pic. 5. *Window of the CIVA software with a curved composite.*

Various applications of this module have been investigated by CEA. Main conclusions drawn from this development is the ability of this hybrid module to simulate new configurations which were not solved yet such as:

- **Study of structural noise due to ultrasonic resonances in pure resin within composite plies** (such features were also previously demonstrated using the FDTD code as a standalone module, but it has been facilitated through parametric settings of the composite structure)
- **Study of ply waviness effects**: the ability to set parameters related to ply waviness (width, height, amplitude) is an innovative new skill which allows predicting induced noise and back wall attenuation due to such waviness within composites.
- **Study of delamination flaws**: It is also possible to add several planar flaws within the simulation configuration, which allows to mimic a delamination after impact damage, which is characterized by successive decohesions at various interplies levels.

Conclusion

This consists in a fully numerical approach of the thermoelastic problem that allows simulating the multi-stacking structure of composite parts with complex shape. A thermal solver has been implemented by the Finite Integration Technique. The increase in the temperature field due to the laser pulse creates thermal stresses in the sample. These thermal stresses are then introduced as a volume source in an elastodynamic FDTD solver. However this approach has its own limitation that consists in taking into account the high frequency content of the ultrasonic waves generated by short laser pulse. Indeed, this needs to decrease drastically the spatial and time meshes giving prohibitive calculation times. We are now working to solve some problems due to numerical instabilities in the coupling method. We are confident that this simulation tool will be of great interest for the simulation of the inspection of composite parts by the laser ultrasonic technique.

References

[1] Davis *et al*., 1997
[2] Dubois M et al. in Review of Progress in QNDE, pp. 529-536, Springer, 1995.
[3] C. B. Scruby and L. Drain, *Laser ultrasonics : techniques and applications*, A. Hilger, 1990.
[4] Rose L R F J. Acoust. Soc. Am. **75** 723 (1984)
[5] Spicer (1991)
[6] McDonald FA Appl. Phys. Lett. **56** 230 (1990)
[7] Sanderson T Ultrasonic **35** 553 (1998)
[8] D. Royer, Elastic Waves in Solids 2: Generation, Acousto-optic Interaction, Application, Springer, 2000.
[9] Weiland T Int. J. Numer. Modell. **9** 295 (1996)
[10] Clemens M, and Weiland T Progress Electromagn. Res **32** 65 (2001).